HHS Public Access

Author manuscript

J Orthop Res. Author manuscript; available in PMC 2019 December 01.

Published in final edited form as:

J Orthop Res. 2018 December ; 36(12): 3231–3238. doi:10.1002/jor.24108.

Computational Simulation of Medial versus Anteromedial Tibial Tuberosity Transfer for Patellar Instability

John J. Elias, PhD[*,1], **Kerwyn C. Jones, MD**[2], **Andrew J. Copa, BS**[1], and **Andrew J. Cosgarea, MD**[3]

[1]Department of Research, Cleveland Clinic Akron General

[2]Department of Orthopedic Surgery, Akron Children's Hospital

[3]Department of Orthopaedic Surgery, Johns Hopkins University

Abstract

The study utilizes dynamic simulation of knee function to determine how tibial tuberosity medialization and anteromedialization influence patellar tracking and contact pressures for knees with patellar instability. Dual limb squatting was simulated with six multibody dynamic simulation models representing knees being treated for patellar instability. Each knee exhibited lateral patellar maltracking in the pre-operative condition based on the bisect offset index. The patellar tendon attachment points on the tibia were medialized by 10 mm to represent tibial tuberosity medialization, with an additional 5 mm of anteriorization applied for anteromedialization. The patellofemoral contact pressure distribution was quantified using discrete element analysis. Data were analyzed with repeated measures analysis of variance with post-hoc tests and linear regressions. Tibial tuberosity medialization and anteromedialization significantly ($p < 0.05$) decreased the bisect offset index for nearly all flexion angles up to 80°, with the largest changes near full extension. Both procedures significantly decreased the maximum lateral pressure at 55°, but increased the maximum medial pressure from 30° to 80°. The pre-operative to post-operative increase in the maximum contact pressure was significantly correlated with the maximum pre-operative bisect offset index for tuberosity medialization ($r^2 = 0.84$), but not for anteromedialization.

Keywords

patellar instability; tibial tuberosity medialization; tibial tuberosity anteromedialization; patellar tracking; cartilage pressure

[*]**Corresponding Author:** John J. Elias, PhD, Cleveland Clinic Akron General, Department of Research, 1 Akron General Ave, Akron, OH 44307, (330) 344-6176, eliasj@ccf.org.

Author contributions

John Elias participated in development of the computational models, running simulations, analyzing data, and preparing the manuscript. Kerwyn Jones and Andrew Cosgarea participated in subject recruitment, study design, and critical evaluation of the manuscript. Andrew Copa participated in model development and validation and preparation of the manuscript. All authors read and approved the final version of the manuscript.

Introduction

For patients with recurrent lateral patellar instability, the lateral position of the tibial tuberosity has been correlated with patellar maltracking[1–4]. Tibial tuberosity osteotomy and medialization alters the orientation of the patellar tendon, decreasing the lateral force acting on the patella. Medialization is often combined with anteriorization (anteromedialization) to decrease patellofemoral compression. Current indications for consideration of tibial tuberosity medialization include lateral patellar maltracking and a lateral position of the tibial tuberosity, typically expressed as a tibial tuberosity to trochlear groove (TT-TG) distance, based on diagnostic imaging, greater than 15 to 20 mm[5–7]. These guidelines are based on limited evidence[6], however.

Previous biomechanical studies have addressed the influence of tibial tuberosity medialization and anteromedialization on patellofemoral function. In vitro simulation studies have generally shown that tibial tuberosity medialization and anteromedialization decrease lateral maltracking and the maximum patellofemoral contact pressure[8–12]. Tuberosity medialization can also increase the pressure applied to cartilage on the medial facet of the patella, however[10], which is a concern for patients with medial cartilage lesions[13]. The previous studies performed with cadaveric knees typically incorporated elevated lateral forces applied to the patella, but did not account for other anatomical characteristics associated with patellar instability, such as trochlear dysplasia and patella alta[14, 15], limiting the clinical relevance of the data.

The current study was performed to characterize how tibial tuberosity medialization and anteromedialization influence patellar tracking and pressure applied to patellofemoral cartilage for symptomatic knees. The study is based on dynamic simulation of function applied to knees being treated for recurrent patellar instability. The study focuses on lateral patellar maltracking as an indicator for tuberosity medialization, regardless of the TT-TG distance. The dynamic simulation technique has previously been assessed for accuracy of simulated patellofemoral kinematics[16, 17]. The current study includes an additional accuracy assessment for the patellofemoral contact pressure distribution.

Methods

Dynamic Simulation of Knee Function

Computational models representing the symptomatic knees of subjects being treated for recurrent lateral patellar instability were used for dynamic simulation of knee function. The models were reconstructed (3D Doctor, Able Software Corp, Lexington, MA and Mimics, Materialise, Leuven, Belgium) from high resolution MRI scans (3.0 T, proton density weighted, slice thickness ranging from 0.6 mm to 1.5 mm). For the current study, a subgroup of the ten existing models were chosen for analysis of tibial tuberosity realignment. The six models chosen exhibited lateral patellar maltracking during simulated knee squatting[17, 18] based on a maximum bisect offset index (portion of the patella lateral to the deepest point of the trochlear groove, Fig. 1) of at least 0.75[19]. The models were reconstructed from 5 females and 1 male. The average age was 16 years (range: 14 to 21 years). The institutional review boards of the two treating institutions provided approval for the study.

The multibody dynamic simulation models (RecurDyn, FunctionBay, Seongnam, Korea) used to represent knee function have been described in detail previously[16–18]. The collateral and cruciate ligaments, patellar tendon, joint capsule, and retinacular structures, including the residual medial retinaculum following injury to the medial patellofemoral ligament, were represented by tension-only springs, with stiffness, damping, and pre-strain at full extension assigned based on previous studies[20–23] (Fig. 1). Quadriceps forces were applied through a representation of the quadriceps tendon to represent the vastus medialis obliquus, vastus lateralis, and combination of the vastus intermedius, rectus femoris, and vastus medialis longus based on previous studies[24, 25]. The vastus medialis obliquus was represented in a weakened state, based on subjects with lateral patellar malalignment[24], by carrying 5% of the total quadriceps force[26]. The femur, tibia and patella and corresponding cartilage surfaces were extracted from the high resolution MRI scans, and cartilage thickness maps were determined based on the distance from elements on the articular surface to the underlying bone. The cartilage surfaces were embedded within the bones for analysis, with the bones treated as rigid structures and patellofemoral and tibiofemoral contact represented by simplified Hertzian contact[27, 28]. Anatomical coordinate systems were fixed to the femur and tibia[29] to characterize tibiofemoral kinematics based on the floating axis convention[30].

Patellofemoral contact pressure distributions were characterized when the patella was within the trochlear groove, using discrete element analysis[16, 31]. Articular reaction forces and moments determined from overlap of cartilage surfaces based on linear elastic theory (discrete element analysis) were balanced against the patellofemoral reaction forces and moments output from multibody dynamic simulation. Starting with the patellofemoral alignment determined from dynamic simulation, the position of the patella was iteratively adjusted to balance the total articular compression force, medial/lateral force and lateral tilt moment applied to the patella between discrete element analysis and multibody dynamic simulation.

Pressure Distribution Accuracy Assessment

Accuracy assessment for the patellofemoral contact pressure distribution compared output from simulations to contact pressure patterns based on in vivo function. Diagnostic imaging captured pre-operative images for all ten knees at three or four positions of knee flexion, spanning the range of patellofemoral contact. Either a dynamic CT scan (Aquilion ONE scanner, Toshiba Medical Systems, Otawara, Japan) acquired images during knee extension against gravity[1, 29] or MRI scans (Magnetom Skyra, Siemens, Munich, Germany) acquired images at multiple positions of knee flexion with resistance applied at the foot as tolerated by the subject[2]. The accuracy of simulated patellofemoral kinematics was previously assessed by comparing computational reconstruction of the imaging data with simulation of the in vivo activity performed by each subject. The simulations reproduced the patellar tracking patterns showing peak lateral tracking near full extension[16] and a decrease in lateral tracking following surgical stabilization[17]. Root mean square errors for pre-operative lateral patellar shift and tilt were 2.7 mm and 3.7°, respectively[17]. For assessment of the patellofemoral contact pressure distribution, femurs and patellas reconstructed from the pre-operative high resolution MRI scans, with attached femoral and patellar cartilage, were shape matched to the bones reconstructed from multiple positions of knee flexion[2]. At each

position of knee flexion for each subject, discrete element analysis was used to determine the contact pressure at each element of the mesh representing the patellar cartilage surface from overlap of the patellar and femoral cartilage surfaces[31].

The motion of each subject during imaging was simulated for comparison of the simulated pressure distribution to the measurements from the subjects[17]. To represent knee extension within the dynamic CT scanner (2 subjects), the femur was fixed in space and quadriceps forces were applied to initiate and maintain extension of the tibia from maximum flexion in the scanner (approximately 45°) to 0°. The total quadriceps force decreased as the knee extended. To represent isometric knee extension within the MRI scanner (8 subjects), models were set at each flexion angle from the MRI scans. With the femur fixed in place, and a force at the foot to match the force applied to each subject, the quadriceps force that maintained the flexion angle was applied. Patellofemoral pressure distributions were determined for each simulation, with the maximum pressure quantified, along with the maximum pressure applied to the lateral and medial facets of the patella.

Tibial Tuberosity Realignment for Simulated Squatting

For assessment of tibial tuberosity medialization and anteromedialization, a dual limb knee squat was simulated for the six patellar maltracking models in the pre-operative condition and following tuberosity realignment. A 200 N body weight was applied to a simulated hip joint that allowed flexion/extension, varus/valgus rotation, and proximal/distal translation. A simulated ankle joint allowed 3 rotational degrees of freedom. The total quadriceps force increased from 42 N at full extension to 300 N at 90º of flexion. To initiate motion, a flexion moment was applied at the hip over the first few degrees of flexion. Tibial tuberosity medialization was represented by shifting the patellar tendon attachment on the tibia medially by 10 mm with the knee extended. Medialization was combined with 5 mm of anteriorization for anteromedialization, representing a tibial osteotomy with low obliquity common for patellar stabilization[7, 32].

Patellar tracking, anatomical parameters, and contact pressure parameters were characterized at 5° intervals of knee flexion. The bisect offset index and patellar lateral tilt were quantified within a plane normal to the long axis of the patella with the posterior condylar axis of the femur oriented horizontally[18]. The TT-TG distance was quantified as the medial-lateral distance from the center of the tibial tuberosity to the deepest point of the trochlear groove[2]. The lateral trochlear inclination (trochlear dysplasia) was measured with the knee at full extension, based on the maximum slope of the lateral ridge of the trochlear groove[18]. The Caton-Deschamps index (alta) was characterized with the knee at 30° of flexion, based on the ratio of the distance from the distal point of the articular surface to the anterior-superior point of the tibia to the length of the articular surface of the patella[18]. The maximum contact pressure and maximum pressure applied to the medial and lateral facets of the patella were quantified from 15° to 90°, when the patella was constrained by the trochlear groove for all knees.

Statistical Analysis

For the pressure distribution accuracy assessment, pressure magnitudes and medial vs. lateral pressure distributions were compared between the reconstruction of in vivo function and simulation of the in vivo motions. The root mean square error for maximum contact pressure was calculated between the simulations and the data from the subjects, including each knee at each flexion angle. For the reconstructed and simulated motions, maximum lateral and medial pressures were compared to each other at the flexion angles closest to 20° and 40° with nonparametric Wilcoxon signed-rank tests. Nonparametric tests were used due to Shapiro-Wilk tests indicating residuals from the comparisons were not normally distributed. Statistical significance was set at $p < 0.05$.

For analysis of the influence of tibial tuberosity realignment on simulated knee squatting, patellar tracking and contact pressures were compared between the tuberosity positions. In addition, changes in the contact pressure distribution following tuberosity realignment were correlated with pre-operative maltracking and lateral position of the tibial tuberosity. The bisect offset index, lateral patellar tilt, and maximum medial and lateral pressures were compared between the tuberosity positions with a repeated measures analysis of variance and post-hoc Student-Newman-Keuls tests, after checking the residuals of the comparisons for non-normal distributions with a Shapiro-Wilk test. Tibial external rotation was also compared as a parameter previously related to tibial tuberosity medialization[29, 33]. Linear regressions were used to correlate the change in maximum pressure due to tuberosity realignment for each knee (ratio of maximum post-operative contact pressure to maximum pre-operative contact pressure) with the maximum pre-operative bisect offset index and TT-TG distance.

Results

The pressure magnitudes and trends in the pressure distribution for simulation of function during diagnostic imaging were similar to those from computational reconstruction of the in vivo function during imaging (Fig. 2). The root mean square error for the maximum cartilage pressure was 1.4 MPa. For the reconstruction of in vivo function, the peak lateral pressure tended to be larger than the peak medial pressure. The difference was statistically significant at 20° ($p = 0.02$), but not at 40° ($p = 0.12$). The peak lateral pressure was significantly larger than the peak medial pressure at both 20° and 40° for the simulations ($p < 0.02$).

For simulated knee squatting, tibial tuberosity realignment decreased lateral patellar tracking and increased tibial external rotation. The average (± standard deviation) pre-operative TT-TG distance with the knee extended was 11 ± 5 mm. The average lateral trochlear inclination was 8° ± 7°. The average Caton-Deschamps index was 1.2 ± 0.1. Patellar lateral tracking was largest near full extension (Table 1). Tuberosity medialization and anteromedialization significantly decreased bisect offset index at nearly all flexion angles, with the average value decreasing by 0.11 for medialization at 0°. Tuberosity medialization and anteromedialization significantly decreased lateral tilt from 10° to 20° of flexion, with a decrease of 3.0° for medialization at 10°. Tuberosity medialization and anteromedialization significantly increased tibial external rotation for all flexion angles (Table 2). The changes

were largest in deep flexion, with an increase of 2.7° at 90° of flexion for tuberosity medialization.

Tuberosity realignment tended to decrease the maximum lateral pressure and increase the maximum medial pressure. The decrease in the maximum lateral pressure was significant for the medialization and anteromedialization conditions at 55° of flexion and for anteromedialization at 85° (Table 3). At 55°, tuberosity medialization and anteromedialization decreased the average maximum lateral pressure by 0.2 MPa. The increase in the maximum medial pressure was statistically significant for the medialization and anteromedialization conditions from 0° to 80°, and also for medialization at 90°. The largest change occurred at 40°, with the average maximum medial pressure increasing by 1.7 MPa for medialization. No significant differences were identified between the medialization and anteromedialization conditions ($p > 0.08$).

Variations in the maximum cartilage pressure due to tuberosity medialization were correlated with pre-operative lateral tracking. The ratio of the maximum post-operative to pre-operative contact pressure decreased as the maximum pre-operative bisect offset index increased ($p < 0.01$, $r^2 = 0.84$, slope = −2.0, Fig. 3), indicating that the increase in maximum pressure was largest for knees with the least pre-operative lateral maltracking. The maximum pressure ratio was not significantly correlated with the maximum pre-operative TT-TG distance for medialization, and no significant relationships were identified with the maximum pressure ratio for anteromedialization ($p > 0.15$).

Discussion

The current results indicate that tibial tuberosity medialization reduces lateral patellar maltracking while shifting contact pressure from the lateral facet of the patella to the medial facet. The decrease in lateral patellar tracking was largest at low flexion angles. Tuberosity anteromedialization tended to produce a greater decrease in the maximum lateral pressure and a smaller increase in the maximum medial pressure, although the flexion angles at which significant differences were noted with respect to the pre-operative condition were similar for medialization and anteromedialization. For tuberosity medialization, the maximum pressure increase was inversely correlated with pre-operative bisect offset index, but not with TT-TG distance. The change in the maximum contact pressure was not significantly correlated with maltracking for anteromedialization.

Previous in vitro testing studies have shown that tibial tuberosity medialization and anteromedialization tend to decrease patellar lateral shift, lateral tilt, and the maximum patellofemoral contact pressure[8–11]. One study indicated that tuberosity medialization did not alter medial contact pressures[8], but two others showed an increase in medial contact pressures[10, 12]. Similar to the current study, previous studies showed non-significant trends for decreased maximum pressures for anteromedialzation, compared to medialization[9, 10].

The current results indicate that tibial tuberosity medialization increases tibial external rotation. One in vitro study[33] and a study based on reconstruction of in vivo function[29] also showed increased tibial external rotation with tuberosity medialization. The current 1° to 3°

increase in external rotation is similar to the change noted from reconstruction of in vivo motion[29]. External rotation moves the tibial tuberosity back toward the pre-operative position, reducing the effective change in the patellar tendon orientation. Each 1° increase in tibial external rotation increases TT-TG distance by approximately 0.5 mm[34]. Increased tibial external rotation will alter tibiofemoral contact points during function, but the influence on tibiofemoral cartilage is currently unknown. Previous computational studies focused on tibial tuberosity medialization or anteromedialization have not accounted for altered tibiofemoral kinematics[35–37].

The current study expands on the previous in vitro and computational studies by representing knees being treated for patellar instability. Each knee demonstrated pre-operative lateral maltracking during simulation of dynamic, closed chain function based on a clinical standard[19]. The average TT-TG distance with the knee extended was 11 mm, which is less than the 15 mm considered a minimum for tuberosity medialization[7]. Measuring TT-TG distance while representing weight-bearing decreased the value compared to the typical unloaded condition, likely by approximately 5 mm[38]. The average lateral trochlear inclination was 8°, indicating a prevalence of trochlear dysplasia for these knees[39]. The average Caton-Deschamps index was 1.2, which is on the borderline of values typically considered an indication of patella alta[40, 41]. Representing pathologic anatomy could contribute to a more dramatic increase in maximum medial pressures for the current study than noted previously.

The data indicates that pre-operative maltracking, rather than TT-TG distance, is the primary parameter determining the efficacy of tibial tuberosity medialization for patellar stabilization. The strong correlation between maximum pressure change and pre-operative maltracking indicates that the medial shift in the patellar pressure distribution could increase the pressure applied to cartilage when the patella is tracking close to the normal range. The medial pressure increase is a particular concern due to the potential for medial cartilage fibrillation and erosion caused by contact between the medial facet of the patella and the lateral condyle of the femur with recurrent instability[42, 43]. Performing anteromedialization rather than medialization tends to reduce pressure increases and eliminates the strong correlation between preoperative tracking and post-operative pressures to provide some protection from overloading cartilage.

The current study further establishes the combination of multibody dynamic simulation and discrete element analysis for representing function typical of patients with patellar instability. Previous studies showed that the multibody dynamic simulation technique produces patellar tracking patterns similar to symptomatic knees, in terms of magnitude of patellar lateral shift and tilt[16, 17], variations with knee flexion[16], and changes due to surgical stabilization[17]. Simulation also produced correlations relating trochlear dysplasia and tibial tuberosity position to patellar tracking similar to relationships determined from subjects[18]. A previous study comparing discrete element analysis output to in vitro pressure measurements showed accurate computational characterization of patellofemoral pressure variations caused by altering the orientation of the patellar tendon[31]. The current study also showed multibody dynamic simulation combined with discrete element analysis produces patellofemoral

contact pressure magnitudes and distributions similar to those based on reconstruction of in vivo motion for symptomatic knees.

Limitations of the study should be noted. Several properties assigned to the models, such as the quadriceps force distribution and elastic properties and initial tension values for springs representing ligaments, tendons, and retinacular structures are assigned based on previously published data, emphasizing the importance of the ongoing accuracy assessment for model output. The sample size was limited by the number of knees that displayed pre-operative lateral maltracking, and the TT-TG distance was not consistently within the range considered for tuberosity medialization. The TT-TG distance was also characterized based on a loaded condition, instead of from unloaded imaging typically used for clinical assessment, since the models were validated and aligned at full extension with application of muscle forces. Future studies could use a larger sample size or manipulation of the tuberosity position to further evaluate the TT-TG distance, since tuberosity position has been correlated with lateral patellar maltracking for computational reconstruction of in vivo function and simulation of knee function[1, 2, 18]. Similar to previous studies[10, 12], tibial tuberosity anteromedialization was represented without changing the quadriceps force based on the moment arm of the patellar tendon about the center of rotation about the knee, although the results were similar to a previous in vitro study with a quadriceps force that varied to balance the flexion moment[9].

Conclusion

Based on the current simulations of dynamic knee squatting, tibial tuberosity medialization performed to treat recurrent patellar instability consistently decreases patellar lateral maltracking, with the largest changes occurring near full extension. Tibial tuberosity medialization can decrease lateral patellofemoral contact pressures, but also increases medial contact pressures. The primary parameter related to elevated post-operative contact pressures following tuberosity medialization is a relatively low level of pre-operative lateral maltracking, rather than a measure of TT-TG distance. Tibial tuberosity anteromedialization lowers, but does not eliminate, the risk of elevated post-operative contact pressures compared to medialization. Further studies focusing on tibial tuberosity medialization with larger levels of pre-operative TT-TG distance are warranted.

Acknowledgement

Research reported in this publication was supported by the National Institute Of Arthritis And Musculoskeletal And Skin Diseases of the National Institutes of Health under Award Number R21AR069150. John Elias is the PI of the grant from the NIH. Andrew Cosgarea has been a board member for the American Orthopaedic Society for Sports Medicine and the Patellofemoral Foundation and has received textbook royalties from Elsevier.

References

1. Elias JJ, Soehnlen NT, Guseila LM, Cosgarea AJ. 2016 Dynamic tracking influenced by anatomy in patellar instability. Knee 23:450–455. [PubMed: 26922799]
2. Biyani R, Elias JJ, Saranathan A, et al. 2014 Anatomical factors influencing patellar tracking in the unstable patellofemoral joint. Knee Surg Sports Traumatol Arthrosc 22:2334–2341. [PubMed: 25063490]

3. Tanaka MJ, Elias JJ, Williams AA, et al. 2015 Correlation between changes in tibial tuberosity-trochlear groove distance and patellar position during active knee extension on dynamic kinematic computed tomographic imaging. Arthroscopy 31:1748–55. [PubMed: 25940399]
4. Williams AA, Elias JJ, Tanaka MJ, et al. 2016 The relationship between tibial tuberosity-trochlear groove distance and abnormal patellar tracking in patients with unilateral patellar instability. Arthroscopy 32:55–61. [PubMed: 26440373]
5. Post WR, Fithian DC. 2018 Patellofemoral instability: A consensus statement from the AOSSM/PFF Patellofemoral Instability Workshop. Orthop J Sports Med. 6:2325967117750352. [PubMed: 29410972]
6. Weber AE, Nathani A, Dines JS, et al. 2016 An algorithmic approach to the management of recurrent lateral patellar dislocation. J Bone Joint Surg Am 98:417–27. [PubMed: 26935465]
7. Duchman K, Bollier M. 2014 Distal realignment: indications, technique, and results. Clin Sports Med 33:517–30. [PubMed: 24993413]
8. Stephen JM, Lumpaopong P, Dodds AL, et al. 2015 The effect of tibial tuberosity medialization and lateralization on patellofemoral joint kinematics, contact mechanics, and stability. Am J Sports Med 43:186–94. [PubMed: 25367019]
9. Ramappa AJ, Apreleva M, Harrold FR, et al. 2006 The effects of medialization and anteromedialization of the tibial tubercle on patellofemoral mechanics and kinematics. Am J Sports Med 34:749–56. [PubMed: 16436533]
10. Saranathan A, Kirkpatrick MS, Mani S, et al. 2012 The effect of tibial tuberosity realignment procedures on the patellofemoral pressure distribution. Knee Surg Sports Traumatol Arthrosc 20:2054–61. [PubMed: 22134408]
11. Ostermeier S, Stukenborg-Colsman C, Hurschler C, Wirth CJ. 2006 In vitro investigation of the effect of medial patellofemoral ligament reconstruction and medial tibial tuberosity transfer on lateral patellar stability. Arthroscopy 22:308–19. [PubMed: 16517316]
12. Beck PR, Thomas AL, Farr J, et al. 2005 Trochlear contact pressures after anteromedialization of the tibial tubercle. Am J Sports Med 33:1710–5. [PubMed: 16093531]
13. Pidoriano AJ, Weinstein RN, Buuck DA, Fulkerson JP. 1997 Correlation of patellar articular lesions with results from anteromedial tibial tubercle transfer. Am J Sports Med 25:533–7. [PubMed: 9240988]
14. Charles MD, Haloman S, Chen L, et al. 2013 Magnetic resonance imaging-based topographical differences between control and recurrent patellofemoral instability patients. Am J Sports Med 41:374–84. [PubMed: 23371940]
15. Steensen RN, Bentley JC, Trinh TQ, et al. 2015 The prevalence and combined prevalences of anatomic factors associated with recurrent patellar dislocation: a magnetic resonance imaging study. Am J Sports Med 43:921–7. [PubMed: 25587185]
16. Elias JJ, Kelly MJ, Smith KE, et al. 2016 Dynamic simulation of the effects of graft fixation errors during medial patellofemoral ligament reconstruction. Orthop J Sports Med 4:2325967116665080. [PubMed: 27709116]
17. Elias JJ, Jones KC, Lalonde MK, et al. 2017 Allowing one quadrant of patellar lateral translation during medial patellofemoral ligament reconstruction successfully limits maltracking without overconstraining the patella. Knee Surg Sports Traumatol Arthrosc. doi:10.1007/s00167-017-4799-9 [Epub ahead of print].
18. Elias JJ, Jones KC, Cyrus Rezvanifar S, et al. 2018 Dynamic tracking influenced by anatomy following medial patellofemoral ligament reconstruction: Computational simulation. Knee 25:262–270. [PubMed: 29544985]
19. Tanaka MJ, Elias JJ, Williams AA, et al. 2016 Characterization of patellar maltracking using dynamic kinematic CT imaging in patients with patellar instability. Knee Surg Sports Traumatol Arthrosc 24:3634–3641. [PubMed: 27358051]
20. Besier TF, Gold GE, Delp SL, et al. 2008 The influence of femoral internal and external rotation on cartilage stresses within the patellofemoral joint. J Orthop Res 26:1627–35. [PubMed: 18524000]
21. Blankevoort L, Kuiper JH, Huiskes R, Grootenboer HJ. 1991 Articular contact in a three-dimensional model of the knee. J Biomech. 24:1019–1031. [PubMed: 1761580]

22. Conlan T, Garth WP, Jr, Lemons JE. 1993 Evaluation of the medial soft-tissue restraints of the extensor mechanism of the knee. J Bone Joint Surg Am 75:682–693. [PubMed: 8501083]
23. Shin CS, Chaudhari AM, Andriacchi TP. 2007 The influence of deceleration forces on ACL strain during single-leg landing: a simulation study. J Biomech. 40:1145–1152. [PubMed: 16797556]
24. Makhsous M, Lin F, Koh JL, et al. 2004 In vivo and noninvasive load sharing among the vasti in patellar malalignment. Med Sci Sports Exerc 36:1768–75. [PubMed: 15595299]
25. Zhang L-Q, Wang G, Nuber GW, et al. 2003 In vivo load sharing among the quadriceps components. J Orthop Res. 21:565–71. [PubMed: 12706033]
26. Elias JJ, Kilambi S, Goerke DR, Cosgarea AJ. 2009 Improving vastus medialis obliquus function reduces pressure applied to lateral patellofemoral cartilage. J Orthop Res 27:578–83. [PubMed: 18985700]
27. Guess TM, Liu H, Bhashyam S, Thiagarajan G. 2013 A multibody knee model with discrete cartilage prediction of tibio-femoral contact mechanics. Comput Methods Biomech Biomed Engin 16:256–270. [PubMed: 21970765]
28. Purevsuren T, Elias JJ, Kim K, Kim YH. 2015 Dynamic simulation of tibial tuberosity realignment: model evaluation. Comput Methods Biomech Biomed Engin 18:1606–1610. [PubMed: 25025488]
29. Elias JJ, Carrino JA, Saranathan A, et al. 2014 Variations in kinematics and function following patellar stabilization including tibial tuberosity realignment. Knee Surg Sports Traumatol Arthrosc 22:2350–2356. [PubMed: 24531362]
30. Grood ES, Suntay WJ. 1983 A joint coordinate system for the clinical description of three-dimensional motions: application to the knee. J Biomech Eng 105:136–144. [PubMed: 6865355]
31. Elias JJ, Saranathan A. 2013 Discrete element analysis for characterizing the patellofemoral pressure distribution: model evaluation. J Biomech Eng 135:81011. [PubMed: 23719962]
32. Liu JN, Steinhaus ME, Kalbian IL, et al. 2017 Patellar Instability Management: A Survey of the International Patellofemoral Study Group. Am J Sports Med. doi: 10.1177/0363546517732045 [Epub ahead of print].
33. Mani S, Kirkpatrick MS, Saranathan A, et al. 2011 Tibial tuberosity osteotomy for patellofemoral realignment alters tibiofemoral kinematics. Am J Sports Med. 39:1024–31. [PubMed: 21233407]
34. Smith BW, Millar EA, Jones KC, Elias JJ. 2018 Variations in tibial tuberosity to trochlear groove and posterior cruciate ligament distances due to tibial external and valgus rotations. J Knee Surg 31:557–561. [PubMed: 28743141]
35. Elias JJ, Cech JA, Weinstein DM, Cosgarea AJ. 2004 Reducing the lateral force acting on the patella does not consistently decrease patellofemoral pressures. Am J Sports Med 32:1202–8. [PubMed: 15262643]
36. Cohen ZA, Henry JH, McCarthy DM, et al. 2003 Computer simulations of patellofemoral joint surgery. Patient-specific models for tuberosity transfer. Am J Sports Med 31:87–98. [PubMed: 12531764]
37. Benvenuti JF, Rakotomanana L, Leyvraz PF, et al. 1997 Displacements of the tibial tuberosity. Effects of the surgical parameters. Clin Orthop Relat Res 343:224–34.
38. Izadpanah K, Weitzel E, Vicari M, et al. 2014 Influence of knee flexion angle and weight bearing on the tibial tuberosity-trochlear groove (TTTG) distance for evaluation of patellofemoral alignment. Knee Surg Sports Traumatol Arthrosc 22:2655–61. [PubMed: 23716013]
39. Carrillon Y, Abidi H, Dejour D, et al. 2000 Patellar instability: assessment on MR images by measuring the lateral trochlear inclination-initial experience. Radiology 216:582–5. [PubMed: 10924589]
40. Magnussen RA, De Simone V, Lustig S, et al. 2004 Treatment of patella alta in patients with episodic patellar dislocation: a systematic review. Knee Surg Sports Traumatol Arthrosc 22:2545–50.
41. Woodmass JM, Johnson NR, Cates RA, et al. 2018 Medial patellofemoral ligament reconstruction reduces radiographic measures of patella alta in adults. Orthop J Sports Med 6:2325967117751659. [PubMed: 29399590]
42. Nomura E, Inoue M. 2004 Cartilage lesions of the patella in recurrent patellar dislocation. Am J Sports Med 32:498–502. [PubMed: 14977680]

43. Salonen EE, Magga T, Sillanpää PJ, et al. 2017 Traumatic patellar dislocation and cartilage injury: A follow-up study of long-term cartilage deterioration. Am J Sports Med 45:1376–1382. [PubMed: 28298062]

Statement of Clinical Significance:

The results indicate tibial tuberosity medialization decreases patellar lateral maltracking and lateral patellofemoral contact pressures, but increases medial contact pressures. When pre-operative patellar maltracking is relatively low, tibial tuberosity medialization is likely to increase maximum contact pressures. Tibial tuberosity anteromedialization lowers the risk of elevated post-operative contact pressures compared to medialization.

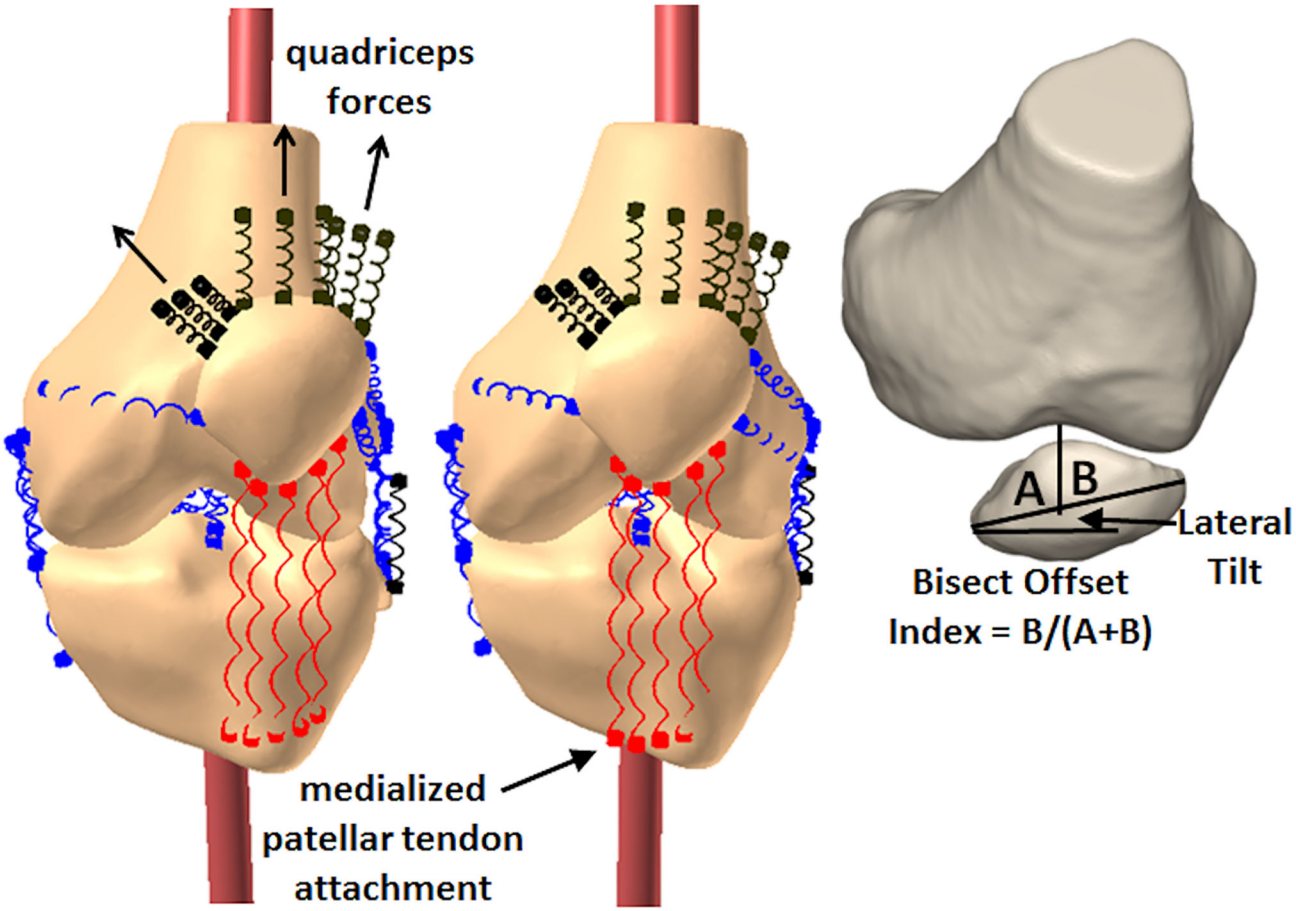

Figure 1:
A computational model showing a knee during dynamic simulation of squatting with the patellar tendon in a pre-operative orientation and following tibial tuberosity medialization. The measures used to characterize patellar tracking are also shown. Adapted from Dynamic tracking influenced by anatomy following medial patellofemoral ligament reconstruction: Computational simulation. [Elsevier] Elias JJ, et al. The Knee (2018). https://doi.org/10.1016/j.knee.2018.02.002 [18].

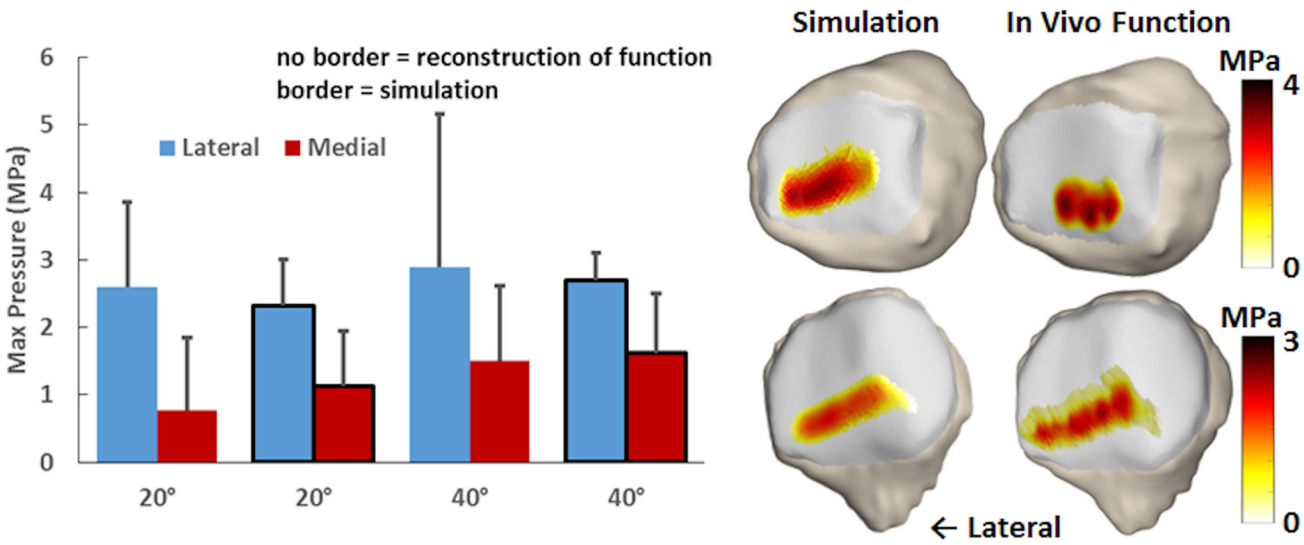

Figure 2:

Average (± standard deviation) maximum lateral and medial pressure for reconstruction of in vivo function and dynamic simulation with the knees at the flexion angles closest to 20° and 40°. Pressure patterns for two knees at approximately 20° are shown for simulation of function and reconstruction of in vivo function.

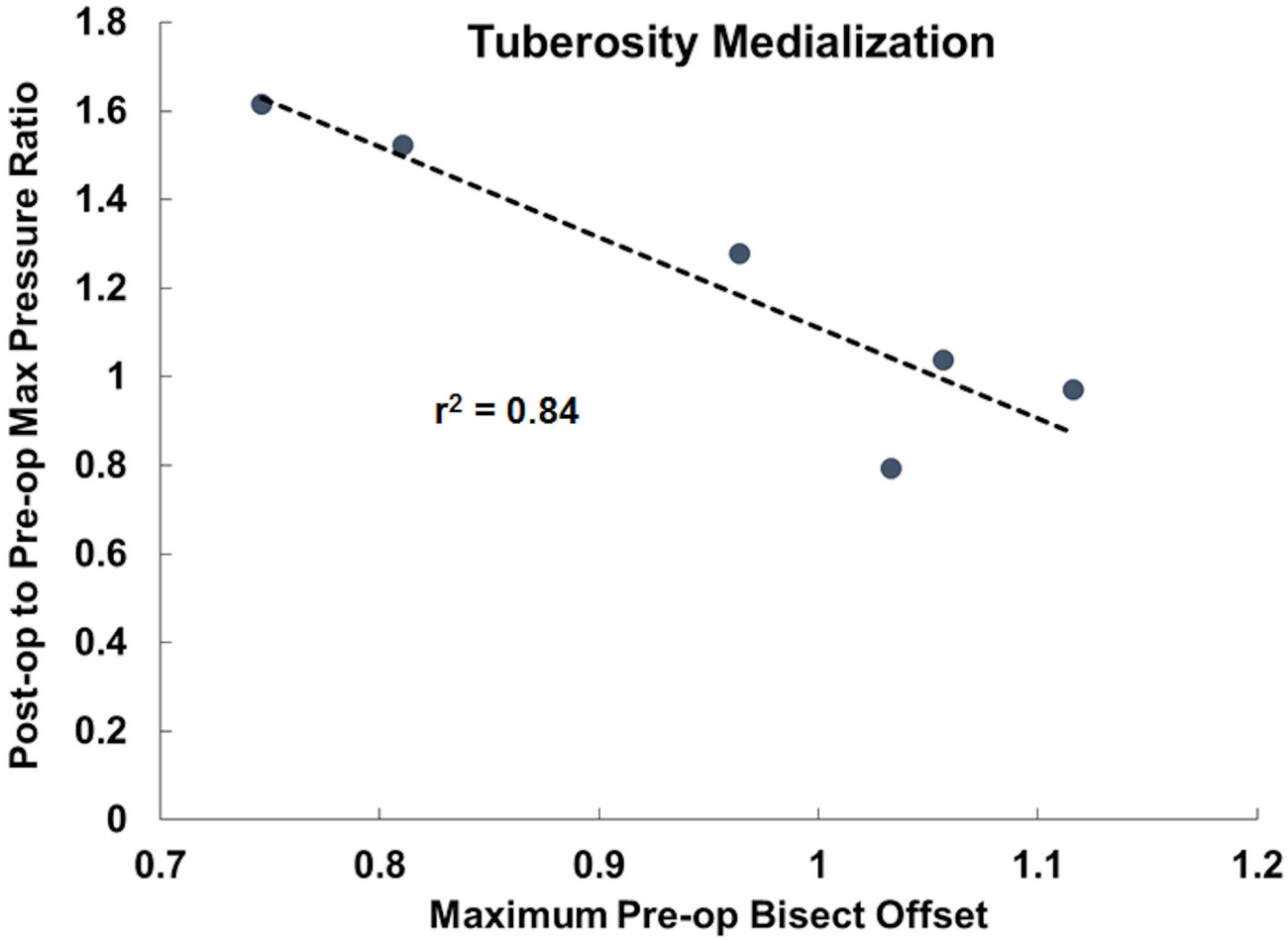

Figure 3:
Variation in the ratio of the maximum post-operative to pre-operative contact pressure with the maximum pre-operative bisect offset index for tuberosity medialization. A best fit line through the data is plotted.

Table 1:

Average ± standard deviation lateral patellar tracking values. Bold font indicates a data point significantly different from the pre-operative condition.

	Bisect Offset Index			Lateral Tilt		
	Pre-Op	**TT med**	**TT amz**	**Pre-Op**	**TT med**	**TT amz**
0°	0.87 ± 0.13	**0.76 ± 0.11**	**0.77 ± 0.11**	18.4 ± 12.6	16.3 ± 9.9	16.5 ± 10.4
5°	0.88 ± 0.11	**0.74 ± 0.07**	**0.74 ± 0.08**	16.9 ± 12.4	15.3 ± 9.8	14.7 ± 9.8
10°	0.84 ± 0.15	**0.71 ± 0.12**	**0.72 ± 0.15**	15.9 ± 11.6	**12.9 ± 9.1**	**13.2 ± 9.7**
15°	0.84 ± 0.16	**0.66 ± 0.14**	**0.67 ± 0.17**	15.1 ± 10.1	**11.6 ± 8.0**	**11.9 ± 8.4**
20°	0.83 ± 0.18	**0.62 ± 0.15**	**0.65 ± 0.14**	14.5 ± 8.8	**10.4 ± 6.9**	**10.4 ± 7.2**
25°	0.82 ± 0.20	**0.60 ± 0.12**	**0.62 ± 0.10**	13.3 ± 8.1	10.0 ± 6.0	9.6 ± 5.8
30°	0.80 ± 0.19	**0.58 ± 0.09**	**0.61 ± 0.09**	12.2 ± 7.9	9.3 ± 5.0	9.1 ± 5.1
35°	0.79 ± 0.18	**0.58 ± 0.09**	**0.59 ± 0.09**	10.9 ± 7.5	9.2 ± 4.7	8.8 ± 4.8
40°	0.76 ± 0.17	**0.58 ± 0.09**	**0.59 ± 0.08**	9.9 ± 7.3	9.2 ± 4.7	8.7 ± 4.8
45°	0.74 ± 0.16	**0.58 ± 0.10**	**0.60 ± 0.07**	8.6 ± 7.0	9.2 ± 4.7	8.5 ± 4.6
50°	0.71 ± 0.14	**0.58 ± 0.09**	**0.60 ± 0.08**	8.1 ± 5.9	9.0 ± 4.6	8.3 ± 4.3
55°	0.67 ± 0.12	**0.59 ± 0.08**	**0.60 ± 0.08**	7.3 ± 4.9	8.4 ± 4.5	8.2 ± 4.1
60°	0.63 ± 0.12	0.59± 0.08	0.60 ± 0.08	8.2 ± 4.9	7.9 ± 4.5	8.0 ± 4.0
65°	0.63 ± 0.12	**0.60 ± 0.09**	**0.59 ± 0.08**	8.0 ± 4.5	7.8 ± 4.3	7.7 ± 4.1
70°	0.62 ± 0.09	**0.59 ± 0.09**	**0.60 ± 0.08**	7.6 ± 4.3	7.6 ± 4.1	7.4 ± 4.1
75°	0.63 ± 0.10	**0.60 ± 0.09**	0.61 ± 0.08	7.4 ± 4.1	7.3 ± 3.9	7.0 ± 4.1
80°	0.62 ± 0.09	**0.59 ± 0.09**	**0.60 ± 0.08**	7.1 ± 4.0	7.0 ± 3.7	6.8 ± 4.0
85°	0.61 ± 0.11	0.59 ± 0.10	0.60 ± 0.09	6.9 ± 3.9	6.7 ± 3.5	6.5 ± 3.8
90°	0.60 ± 0.09	0.58 ± 0.10	0.61 ± 0.08	6.6 ± 3.7	6.5 ± 3.3	6.2 ± 3.8

Pre-op: Pre-operative condition, TT med: Tibial tuberosity medialization,

TT amz: Tibial tuberosity anteromedialization

Table 2:

Average ± standard deviation tibial external rotation. Bold font indicates a data point significantly different from the pre-operative condition.

	External Rotation		
	Pre-Op	**TT med**	**TT amz**
0°	5.8 ± 3.4	**6.2 ± 3.3**	**6.2 ± 3.3**
5°	6.3 ± 3.5	**7.1± 3.7**	**7.2 ± 3.4**
10°	6.6 ± 4.2	**7.8 ± 3.9**	**7.8 ± 3.9**
15°	6.5 ± 4.6	**7.9 ± 4.3**	**8.1 ± 4.2**
20°	6.3 ± 4.7	**7.7 ± 4.2**	**8.1 ± 4.1**
25°	5.8 ± 4.7	**7.4 ± 4.0**	**7.8 ± 3.9**
30°	5.5 ± 5.1	**7.1± 4.2**	**7.6 ± 4.2**
35°	5.2 ± 5.6	**6.9 ± 4.7**	**7.5 ± 4.6**
40°	5.2 ± 6.0	**7.1 ± 4.9**	**7.7 ± 4.9**
45°	5.4 ± 6.4	**7.4 ± 5.3**	**8.1 ± 5.4**
50°	5.7 ± 6.9	**7.8 ± 6.0**	**8.6 ± 6.0**
55°	6.0 ± 7.6	**8.3 ± 6.6**	**9.1 ± 6.7**
60°	6.2 ± 8.3	**8.9 ± 7.3**	**9.6 ± 7.4**
65°	6.5 ± 9.1	**9.3 ± 8.1**	**10.0 ± 8.2**
70°	6.8 ± 9.8	**9.6 ± 8.8**	**10.3 ± 8.9**
75°	6.9 ± 10.4	**9.8 ± 9.5**	**10.4 ± 9.5**
80°	7.2 ±10.9	**10.0 ± 10.0**	**10.5 ± 10.1**
85°	7.5 ± 11.2	**10.3 ± 10.5**	**10.8 ± 10.5**
90°	7.9 ± 11.4	**10.6 ± 10.7**	**11.1 ± 10.7**

Pre-op: Pre-operative condition, TT med: Tibial tuberosity medialization,

TT amz: Tibial tuberosity anteromedialization

Table 3:

Average ± standard deviation maximum medial and lateral pressures. Bold font indicates a data point significantly different from the pre-operative condition.

	Maximum Lateral Pressure			Maximum Medial Pressure		
	Pre-Op	**TT med**	**TT amz**	**Pre-Op**	**TT med**	**TT amz**
15°	2.5 ± 0.7	2.6 ± 0.9	2.6 ± 0.9	0.5 ± 1.4	1.4 ± 2.4	0.8 ± 2.1
20°	2.7 ± 0.5	3.0 ± 1.2	2.5 ± 0.6	0.7 ± 1.4	1.1 ± 2.1	1.4 ± 1.9
25°	3.0 ± 0.5	2.9 ± 0.9	2.6 ± 0.5	0.8 ± 1.2	2.0 ± 1.0	1.5 ± 1.5
30°	3.2 ± 0.6	2.9 ± 0.9	2.7 ± 0.6	0.8 ± 1.1	**2.3 ± 1.5**	**1.8 ± 1.3**
35°	3.3 ± 0.6	3.1 ±0.8	2.6 ± 0.5	0.9 ± 1.1	**2.6 ± 1.1**	**2.2 ± 0.6**
40°	3.4 ± 0.8	3.0 ± 0.7	2.6 ± 0.5	1.0 ± 1.2	**2.7 ± 0.8**	**2.3 ± 0.6**
45°	3.3 ± 0.8	3.1 ± 0.8	2.8 ± 0.5	1.1 ± 1.1	**2.8 ± 0.7**	**2.3 ± 0.5**
50°	3.3 ± 0.7	3.2 ± 0.8	2.8 ± 0.6	1.2 ± 1.2	**2.8 ± 0.6**	**2.3 ± 0.5**
55°	3.1 ± 0.5	**2.9 ± 0.6**	**2.9 ± 0.5**	1.3 ± 1.1	**2.6 ± 0.4**	**2.4 ± 0.5**
60°	3.1 ± 0.6	2.9 ± 0.7	2.9 ± 0.7	1.8 ± 0.6	**2.5 ± 0.4**	**2.4 ± 0.4**
65°	3.0 ± 0.7	3.0 ± 0.8	2.9 ± 0.7	1.8 ± 0.5	**2.6 ± 0.3**	**2.4 ± 0.5**
70°	3.1 ± 0.7	3.1 ± 0.9	3.0 ± 0.8	1.9 ± 0.5	**2.7 ± 0.5**	**2.6 ± 0.7**
75°	3.1 ± 0.7	3.1 ± 0.8	3.1 ± 0.8	2.1 ± 0.6	**2.9 ± 0.7**	**2.8 ± 0.9**
80°	3.1 ± 0.6	3.1 ± 0.6	3.0 ± 0.6	2.2 ± 0.6	**3.0 ± 0.9**	**3.0 ± 1.1**
85°	3.1 ± 0.5	3.0 ± 0.5	**2.8 ± 0.4**	2.6 ± 0.8	3.2 ± 1.2	3.1 ± 1.3
90°	3.0 ± 0.4	2.9 ± 0.5	2.9 ± 0.4	2.7 ± 1.1	**3.3 ± 1.2**	3.2 ± 1.6

Pre-op: Pre-operative condition, TT med: Tibial tuberosity medialization,

TT amz: Tibial tuberosity anteromedialization